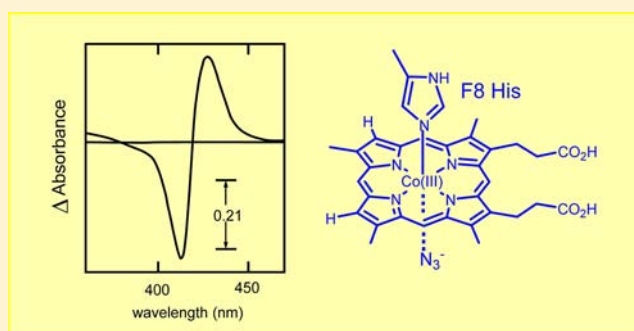


## Relaxation Analysis of Ligand Binding to the Myoglobin Reconstituted with Cobaltic Heme

Saburo Neya,<sup>\*,†</sup> Masaaki Suzuki,<sup>†</sup> Tyuji Hoshino,<sup>†</sup> and Akira T. Kawaguchi<sup>‡</sup><sup>†</sup>Department of Physical Chemistry, Graduate School of Pharmaceutical Sciences, Chiba University, Chuoh-Inohana, Chiba 260-8675, Japan<sup>‡</sup>School of Medicine, Tokai University, Isehara, Kanagawa 259-1193, Japan

## Supporting Information

**ABSTRACT:** Myoglobin reconstituted with oxidized Co(III) deuteroheme was found to exhibit relatively large affinities to  $\text{CN}^-$ ,  $\text{N}_3^-$ ,  $\text{SCN}^-$ , pyridine, and imidazole contrary to the early proposal. The ligand-induced changes in electronic spectra were less obvious than those of Fe(III) myoglobin owing to the absence of accompanied spin-state transition on the ligand binding. The relaxation kinetic analysis revealed that the ligand association rates were small and that the dissociation rates were still much smaller. The relatively large ligand affinities in Co(III) myoglobin were found due to the compensation of small association rates with fairly smaller dissociation rates. This is in marked contrast with the ligation profile in Fe(III) myoglobin where large association rates and small dissociation rates are generally observed. The rationale for the characteristic ligand-binding behavior of Co(III) myoglobin was provided on the basis of the properties of Co(III) which has an additional negative charge and forms stronger metal–ligand bonds than Fe(III).



## INTRODUCTION

Hemoproteins exhibit distinctly different functions such as reversible oxygen binding, oxygen reduction to water, electron transfer, and drug metabolism. Replacement of the iron in hemoproteins with metal ions such as copper, manganese, and zinc has been widely utilized to perturb the biochemical function of hemoproteins. Hoffman and Dickerson have reviewed the metal substitution results in hemoglobin, myoglobin (Mb), and cytochrome *c*.<sup>1,2</sup> Among metal substituted hemoproteins, one of the most successful examples is found in cobalt-bearing hemoproteins. Cobaltous or Co(II) heme not only reversibly binds oxygen, but also the deoxy- and oxy-Co(II) hemes are active to electron paramagnetic resonance (EPR).<sup>3,4</sup> This is in marked contrast with Fe(II) hemoprotein which is EPR-silent in both of the oxy and deoxy states. Yonetani and his co-workers exquisitely applied EPR to the structural analysis of Co(II) Mb and Co(II) hemoglobin.<sup>5,6</sup> They furthermore revealed the ligation pathway of oxygen to the constituting subunits within intact hemoglobin with the [Co(II), Fe(II)] hybrids.<sup>7</sup>

Compared with Co(II) hemoproteins, the analyses of cobaltic or Co(III) hemoprotein have been rather limited. Ridsdale et al. reported that Co(III) hemoglobin adopts an internal hemichrome with ligation of both the proximal and distal histidines to Co(III).<sup>8</sup> The crystal structures of Co(III) Mb were reported by Brucker et al. in 1996 and by Zahran et al. in 2008; a water molecule was found as the sixth coordination ligand in Co(III) Mb.<sup>9,10</sup> Accordingly, the old claim that

hemichrome structure prevents the binding of exogenous ligands such as  $\text{OCN}^-$ ,  $\text{SCN}^-$ ,  $\text{F}^-$ ,  $\text{N}_3^-$ , and pyridine<sup>8,11</sup> for Co(III) hemoglobin seems not always adequate. It is likely that another factor to control the ligand binding to Co(III) hemoprotein is present. For a bacterial Co(III) hemoprotein, Moura and co-workers noted a slight spectral shift upon the  $\text{CN}^-$  addition.<sup>12</sup> Yoshida and Kikuchi reported that  $\text{N}_3^-$  and  $\text{CN}^-$  do not change the visible spectrum of Co(III)–heme bound heme oxygenase, suggesting that these ligands do not bind to the Co(III)-replaced enzyme.<sup>13</sup> Heinecke and co-workers recently analyzed the slow nitrite binding to Co(III) Mb to explore the nitrite reductase activity.<sup>14</sup>

The basic aspects of ligand binding to Co(III) Mb have not been fully explored; neither the kinetic parameter nor the equilibrium constant has been reported except for the nitrite case.<sup>14</sup> This is because the complex formation of Co(III) hemoprotein is so slow that one cannot readily follow the complete equilibration. In view of the continuing interest in Co(III)-substituted hemoproteins,<sup>8–14</sup> the binding analysis for common ligands such as  $\text{CN}^-$  and  $\text{N}_3^-$  to Co(III) hemoprotein will still be important. We consequently started to characterize the ligation profile of familiar anionic and neutral ligands to Co(III) Mb. The heme employed in our work was deuteroheme (Figure 1), rather than protoheme, because the heme protons at 2,4-positions were expected to show large

Received: January 12, 2013

Published: June 12, 2013

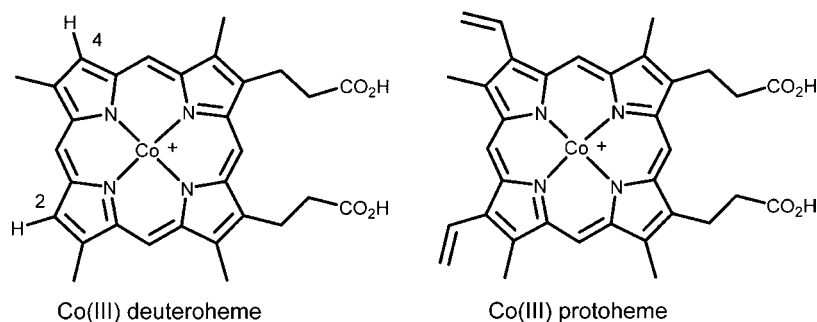


**Figure 1.** Structure of the prosthetic groups. Co(III) deuteroheme was used in this work. The axial ligand of Co(III) is omitted for clarity.

chemical shifts in the paramagnetic nuclear magnetic resonance (NMR) spectrum, and because the NMR signals may serve as spin-state markers.<sup>15</sup> We demonstrate herein that careful analyses with visible absorption and proton NMR reveal the unrecognized ligand-binding profile of Co(III) Mb. The uniqueness of Co(III) Mb as compared with Fe(III) Mb will be discussed on the basis of these results.

## MATERIALS AND METHODS

**Synthesis of Prosthetic Group.** Fe(III) protohemin (Tokyo Chemical Industry, Tokyo) was converted to deuterohemin with the resorcinol-melt procedure, and transformed to the dimethylester in methanol containing 5% sulfuric acid.<sup>16</sup> Demetalated deuteroporphyrin dimethylester was prepared with the iron-powder treatment.<sup>16</sup> The identity of resulting deuteroporphyrin was confirmed with proton NMR.<sup>17</sup> Co(II) was inserted to the porphyrin in refluxing *N,N*-dimethylformamide under argon atmosphere in the presence of Co(II) acetate,<sup>18</sup> and the Co(II) heme was purified by silica-gel column chromatography with chloroform eluent. The chloroform solution of Co(II) deuteroheme dimethylester was mixed with an equal volume of 0.5 M NaCl dissolved in aqueous 0.1 M HCl, and allowed to stir overnight at room temperature to oxidize into Co(III)Cl deuteroheme dimethylester. A 100 mg of Co(III)Cl deuteroheme dimethylester, obtained after chloroform evaporation, was dissolved in a methanol (50 mL)/water (5 mL) mixture containing 3.0 g of KOH, and the solution was refluxed overnight to hydrolyze the ester side chains. The cooled solution, diluted with an equal volume of water, was treated with 36% aqueous HCl saturated with NaCl to precipitate Co(III)Cl deuteroheme bearing free acid chains (Figure 1). The precipitate was collected, washed with a small volume of water on a centrifuge, and dried at 50 °C in an oven.

**Reconstituted Mb.** ApoMb was prepared from sperm whale Mb (Sigma, Type II) with the acid–butanone method.<sup>19</sup> Mb was reconstituted with Co(III) deuteroheme after Yonetani et al., and purified with the CM-cellulose (Whatman, CM52) column chromatography.<sup>5</sup> Concentration of Co(III) deuteroheme Mb was determined with an extinction coefficient  $\epsilon_{415} = 128 \text{ mM}^{-1} \text{ cm}^{-1}$  on the basis of pyridine-hemochromism spectrum of Co(III) deuteroheme with  $\epsilon_{415} = 130 \text{ mM}^{-1} \text{ cm}^{-1}$ .<sup>5</sup> The pH of Mb solution was monitored with a Toko pH meter TP-8. Tris(hydroxymethyl)aminomethane (Tris), D<sub>2</sub>O, and ligand molecules (KCN, NaN<sub>3</sub>, KSCN, pyridine, and imidazole) were purchased from Wako Pure Chemical Industries, Osaka, and used as received.

**Physical Measurements.** Electronic absorption spectra were recorded at 20 °C on a Shimadzu MPS-2000 spectrophotometer with a thermostatted cell-holder connected with a temperature controlling unit. Proton NMR spectra at 600 MHz were obtained with a JEOL ECA-600 spectrometer. The chemical shift was referenced against sodium 2,2-dimethyl-2-silapentane-5-sulfonate (DSS).

## RESULTS

**Overview of Electronic Absorption Spectra.** Figure 2 shows the optical absorption spectrum of the Mb reconstituted

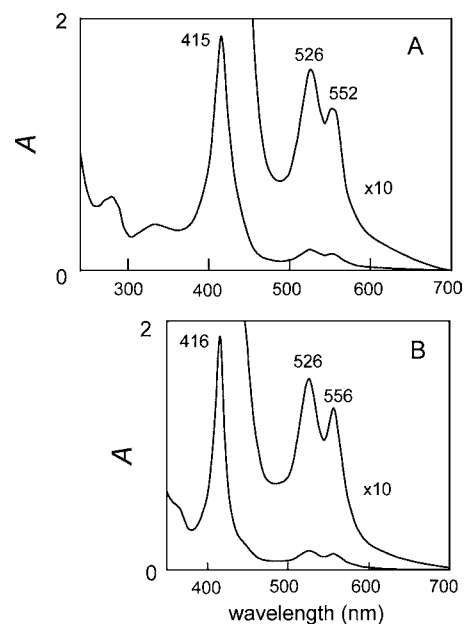


**Figure 2.** Electronic absorption spectra. (A) Co(III) Mb in 0.1 M Tris at pH 7.0 and 20 °C. (B) Co(III) deuteroheme dimethylester at 20 °C in dichloromethane containing 0.3 M of 1-methylimidazole.

with Co(III) deuteroheme. The Soret band at 415 nm was 3.1-fold higher than the 280-nm protein band, and the visible peak maxima were found at 552 ( $\alpha$  band) and 526 ( $\beta$  band) nm. Since Co(III) hemoglobin has been proposed to have an internal hemichrome,<sup>8,9</sup> Co(III) Mb is likely to adopt a similar coordination structure. So, we recorded the spectrum of a “model compound” of *bis*-coordinated with 1-methylimidazole to explore the possibility. The visible spectrum of the model heme with peaks at 416, 526, and 556 nm in Figure 2 was similar to that of the Co(III) Mb although the 552-nm peak is slightly less intense in Mb. Yonetani and co-workers reported that the *bis*-pyridine complex of Co(III) deuteroheme exhibited an optical spectrum with peaks at 415, 525, and 556 nm, which was also closely similar to that of the *bis*-imidazole complex in Figure 2.<sup>5</sup> From the apparent spectral similarity between Co(III) Mb and the model compounds with *bis*-1-methylimidazole or *bis*-pyridine, one may guess the hemichrome-structure for Co(III) Mb.<sup>8,9</sup>

**Ligand Binding to Co(III) Mb.** It has been suggested that N<sub>3</sub><sup>−</sup> does not coordinate to Co(III) hemoproteins.<sup>1,8,11</sup> On careful examination of the Soret difference spectra, however, we observed appreciable optical changes after addition of N<sub>3</sub><sup>−</sup> to Co(III) Mb. Figure 3A shows the time-dependent transition induced by N<sub>3</sub><sup>−</sup>. The difference spectra showed a minimum at

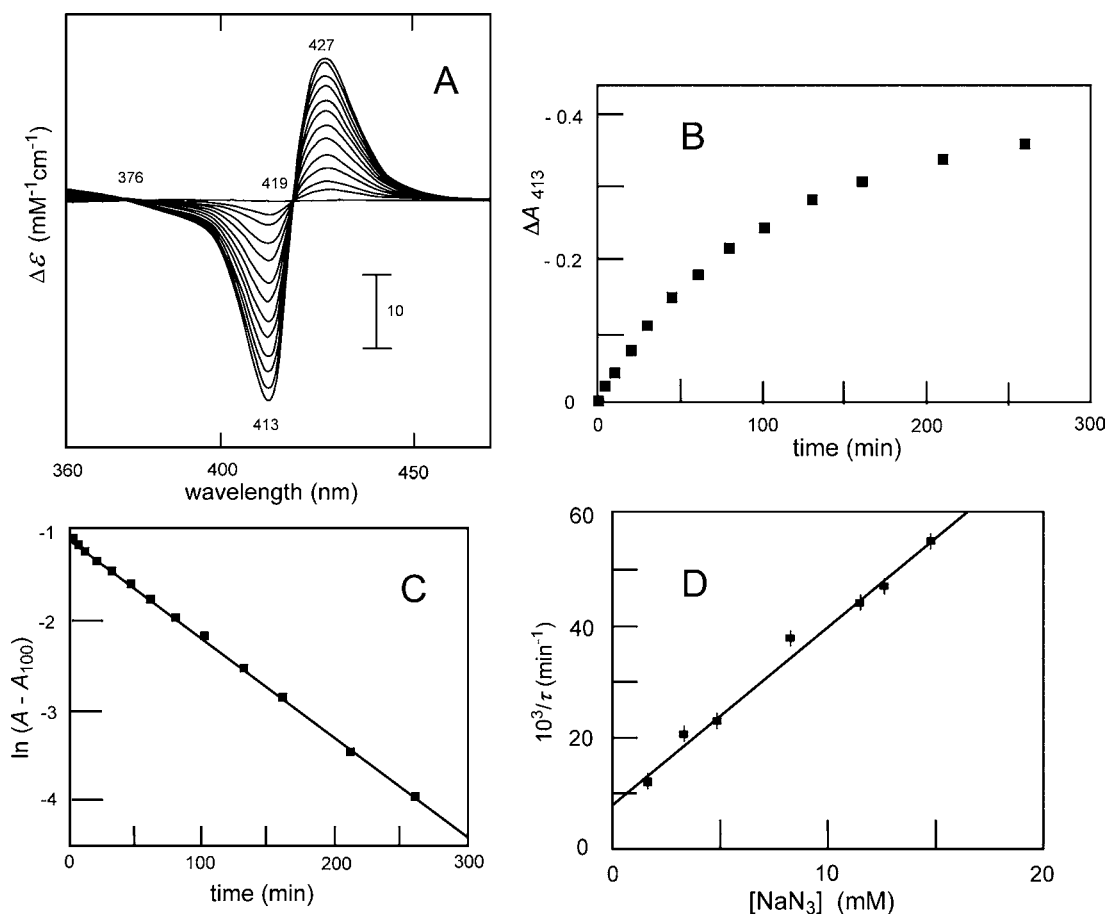


**Figure 3.** Optical changes of Co(III) deuteroheme Mb by  $\text{N}_3^-$ . (A) Soret absorption transition induced by 1.46 mM of  $\text{N}_3^-$  in 0.1 M Tris at pH 7.0 and 20 °C. Heme concentration was 14  $\mu\text{M}$ . The transitions over 260 min were recorded. (B) Time progress of optical changes in (A). (C) Analysis of the spectral transitions in (B). (D) Dependence of the relaxation rate on azide concentration.

413 nm and a maximum at 427 nm with the isosbestic points at 376 and 419 nm. The progress was so slow that it took about two hours to go halfway of the equilibration (Figure 3B). The transition, although rather sluggish, suggests that  $\text{N}_3^-$  ion coordinates to Co(III) Mb.

**Relaxation Analysis of  $\text{N}_3^-$  Binding.** Figure 3B shows the time process of the optical decrease at 413 nm in Co(III) Mb on the  $\text{N}_3^-$  binding. Since the exponential decay progressed very slowly over several hours, we could not estimate the binding constant with the conventional plots of  $(1/[\text{N}_3^-], 1/\Delta A)$ .<sup>20</sup> The observation suggested that the forward- and backward-processes competed against each other with long time scales. We analyzed the results in Figure 3B with the transient relaxation kinetics according to the scheme in eq 1:



where Mb and L denote Co(III) Mb and exogenous ligand, respectively, and  $k_{\text{on}}$  and  $k_{\text{off}}$  are the rate constants. The observed rate constant  $1/\tau$  or relaxation time  $\tau$  is given by eq 2.<sup>21</sup>

$$1/\tau = k_{\text{on}} + k_{\text{off}}[\text{N}_3^-] \quad (2)$$

Relaxation analysis has been generally applied to extremely fast processes. However, since there is no limitation to relaxation time, the analysis is applicable to slow reactions as well. In the observation of Figure 3B, the final absorbance  $A_{100}$

was recorded 5 h after addition of 1.64 mM of  $\text{N}_3^-$ . A good linear correlation between time and  $\log\Delta A$ , where  $\Delta A = A - A_{100}$ , was observed, as indicated in Figure 3C, and we obtained a slope corresponding to a relaxation time  $\tau = (1.17 \pm 0.09) \times 10^{-2}$  min. Figure 3D shows the dependence of apparent rate constant on the ligand concentration. The relaxation rate was found to increase linearly with increasing  $\text{N}_3^-$  concentration. From the linear plots analyzed with eq 2, the values of  $k_{\text{on}} = (5.2 \pm 1.0) \times 10^{-2} \text{ M}^{-1} \text{ s}^{-1}$  and  $k_{\text{off}} = (1.4 \pm 0.3) \times 10^{-4} \text{ s}^{-1}$  were obtained. The binding constant for  $\text{N}_3^-$  was  $K = k_{\text{on}}/k_{\text{off}} = 370 \pm 150 \text{ M}^{-1}$ .

**Binding of Pyridine, Imidazole,  $\text{SCN}^-$ , and  $\text{CN}^-$ .** Contrary to the earlier observation that only  $\text{CN}^-$  and nitrite bind to Co(III) hemoproteins,<sup>1,8,11,14</sup> we found that several other ligands react with Co(III) Mb. The binding of pyridine, imidazole, and  $\text{SCN}^-$  occurred over 2–5 h, as with the case for  $\text{N}_3^-$ , and relatively large changes were obtained. Figure 4 illustrates the Soret difference spectra induced by these ligands.

Troughs around 410 nm and peaks near 420 nm were commonly noted with the minor differences in the peak position and peak shape. These spectra suggest the ligand coordination. The time-course of transition was exponential, and the relaxation rates were estimated similarly as for the  $\text{N}_3^-$  ligation. Figure 5 summarizes the relationship between the relaxation rates and ligand concentrations, from which the  $k_{\text{on}}$  and  $k_{\text{off}}$  were estimated. The results were compiled in Table 1.

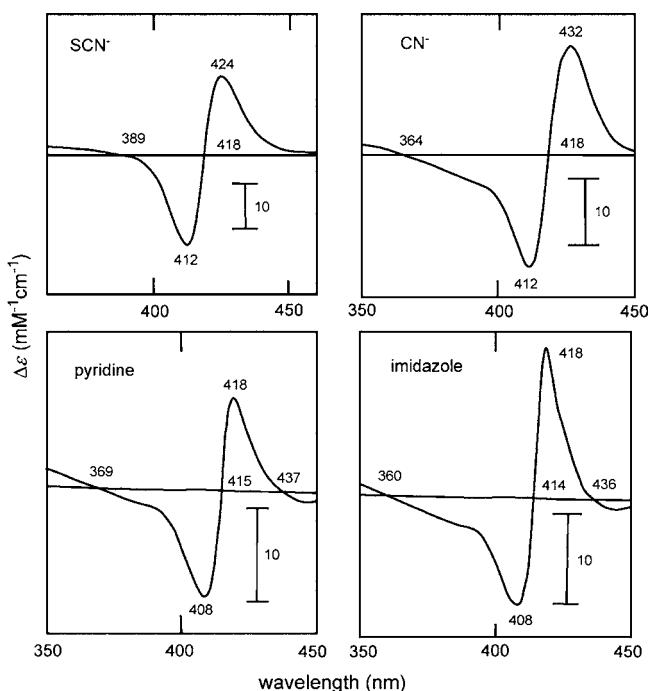


**Figure 4.** Ligand-induced Soret difference spectra of Co(III) Mb in 0.1 M Tris at pH 7.0 and 20 °C. Ligand concentrations are  $[\text{SCN}^-] = 120 \mu\text{M}$ ,  $[\text{CN}^-] = 98 \mu\text{M}$ ,  $[\text{pyridine}] = 1.0 \text{ mM}$ , and  $[\text{imidazole}] = 2.9 \text{ mM}$ . The spectra were recorded 5 h after addition of the ligands.

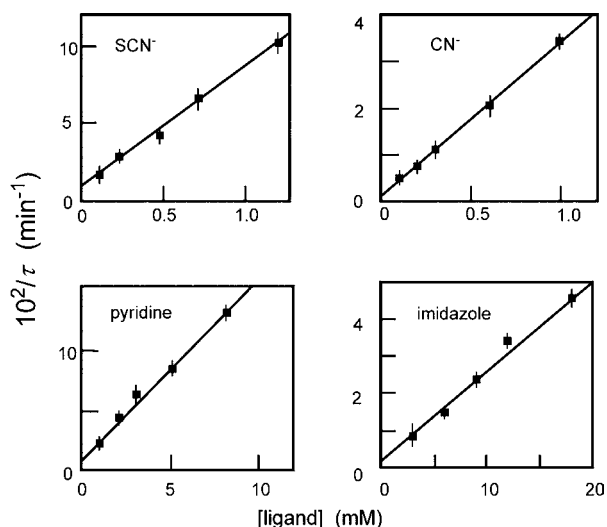


**Figure 5.** Plots of relaxation rates and ligand concentrations of the anionic and neutral ligands. The solid lines represent the least-squares fit. Co(III) Mb was in 0.1 M Tris buffer at pH 7.0 and 20 °C.

We also examined the binding of fluoride  $\text{F}^-$  to Co(III) Mb, but no significant optical change was observed.

Figure 6 compares the visible spectra among the Co(III) Mb complexes. The overall features with the dominant  $\alpha$  and  $\beta$  bands around 560 and 540 nm and without the charge-transfer peaks around 500 and 630 nm are analogous to each other. The spectra in the Soret region also looks similar to each other. Soret bands were centered on  $\sim 415 \text{ nm}$ , and the Soret peak widths at a half-height were 30–33 nm for all of the derivatives (results not shown). The spectral data of the Co(III) Mb compounds are summarized in Table 2.

**Acid–Alkaline Transition of Co(III) Mb.** We examined the pH-dependent visible spectra of Co(III) deuteroheme Mb to identify the ligand at the sixth coordination site. With increasing pH from 7 to 10, small but appreciable changes were observed as illustrated in Figure 7. The spectral shift was fully reversible. Monitoring the absorbance development at 540 nm, we obtained the midpoint of transition at  $\text{pH} = 8.70 \pm 0.11$ . We also analyzed the pH-dependent spectra of Co(III) protoheme Mb; similar transitions were observed (Figure S1 in Supporting Information [SI]). The peaks maxima and isosbestic points of the spectra in Co(III) protoheme Mb were shifted to red by 5–7 nm as compared with those of Co(III) deuteroheme Mb. This is expected from increased  $\pi$  electron system in protoheme. The  $\text{pK}$  of the acid-alkaline transition of Co(III) protoheme Mb was  $8.56 \pm 0.13$  (Figure S1 in SI).

**Proton NMR Spectroscopy.** Co(III) Mb with six 3d-electrons could be in either high-spin ( $S = 2$ ) or low-spin ( $S = 0$ ) state. We recorded the proton NMR spectrum of Co(III) Mb in the absence of external ligand to identify the spin state of the Co(III) ion. In the spectrum recorded over a  $\pm 100 \text{ ppm}$  region, we found only the protein signals in a regular 0–10 ppm region, but no hyperfine-shifted signal was observed (Figure S2 in SI).

## DISCUSSION

**Coordination State of Co(III) Deuteroheme Mb.** The hemoproteins containing Co(III) heme have been suggested not to bind exogenous ligand except for  $\text{CN}^-$  and nitrite.<sup>1,8,12,13</sup> The spectral similarity between Co(III) Mb and the Co(III) heme with two axial 1-methylimidazoles (Figure 2) may suggest that Co(III) Mb is “acid denatured” like Co(III) hemoglobin.<sup>1,8</sup> However, care must be taken in the interpretation of the spectral similarity. Careful examination of the Soret difference spectra in Figure 4 indicates that the exogenous ligands such as  $\text{N}_3^-$ ,  $\text{SCN}^-$ , pyridine, and imidazole bind to Co(III) Mb.

The visible spectrum of Co(III) Mb without added ligand is indeed anomalous in comparison with that of Fe(III) hemoproteins. Native Mb and P450 without external ligands exhibit enhanced charge-transfer bands around 500 and 630 nm, and the weaker  $\alpha$  and  $\beta$  peaks.<sup>22,23</sup> Soret maxima of Fe(III) Mb and P450 are located at 405 and 391 nm, respectively.<sup>22,23</sup> By contrast, Co(III) Mb in the absence of exogenous ligand shows no charge-transfer bands, and the Soret maximum is red-shifted to 415 nm (Table 2). However, the ligand affinities of Co(III) Mb are moderately large as indicated in Table 1. We accordingly suggest that the Co(III) deuteroheme Mb is not a hemochrome compound but the coordination site is occupied with a water molecule. Hambright et al. from the detailed reduction analysis assumed the aquomet structure for Co(III) protoheme Mb,<sup>11</sup> and the X-ray analyses by the groups of Brucker et al. and Zahran et al. verified the assumption.<sup>9,10</sup> Our suggestion for the aquomet structure in Co(III) deuteroheme Mb is supported from the pH-dependent spectra in Figure 6. The acid-alkaline transition of the Mb occurred at pH 8.7 (Figure 7), which is close to pH 8.8 in aquomet Fe(III) deuteroheme Mb.<sup>24</sup> We analyzed the transition of aquomet Co(III) protoheme Mb as well (Figure S1 in SI). The  $\text{pK} = 8.56$  of Co(III) protoheme Mb was close to  $\text{pK} = 8.7$  of Fe(III) protoheme Mb.<sup>24</sup> The results for the two types of Co(III) Mb indicate that the normal Co(III)– $\text{H}_2\text{O}$ –N(distal histidine) linkages, similar to those in Fe(III) Mbs, are retained at the heme distal site.

Table 1. Rate and Equilibrium Constants for Ligand Binding of Co(III) Mb and Fe(III) Mb

heme	ligand	$k_{\text{on}}$ ( $\text{M}^{-1} \text{s}^{-1}$ )	$k_{\text{off}}$ ( $\text{s}^{-1}$ )	$K$ ( $\text{M}^{-1}$ )	reference
deuteroCo(III)	$\text{N}_3^-$	$(5.2 \pm 1.0) \times 10^{-2}$	$(1.4 \pm 0.3) \times 10^{-4}$	$(3.7 \pm 1.5) \times 10^2$	this work
deuteroCo(III)	$\text{CN}^-$	$(5.6 \pm 0.9) \times 10^{-2}$	$(2.0 \pm 0.4) \times 10^{-6}$	$(2.8 \pm 1.0) \times 10^4$	this work
deuteroCo(III)	$\text{SCN}^-$	$1.3 \pm 0.2$	$(1.4 \pm 0.3) \times 10^{-4}$	$(9.3 \pm 3.0) \times 10^3$	this work
deuteroCo(III)	imidazole	$(4.4 \pm 0.6) \times 10^{-2}$	$(9.1 \pm 0.8) \times 10^{-6}$	$(4.8 \pm 1.1) \times 10^2$	this work
deuteroCo(III)	pyridine	$(2.3 \pm 0.3) \times 10^{-1}$	$(2.4 \pm 0.4) \times 10^{-4}$	$(9.6 \pm 2.9) \times 10^2$	this work
heme	ligand	$k_{\text{on}}$ ( $\text{M}^{-1} \text{s}^{-1}$ )	$k_{\text{off}}$ ( $\text{s}^{-1}$ )	$K$ ( $\text{M}^{-1}$ )	reference
protoFe(III)	$\text{N}_3^-$	$7.0 \times 10^3$	$4.9 \times 10^{-1}$	$1.4 \times 10^4$	ref 37
protoFe(III)	$\text{CN}^-$	$1.7 \times 10^2$	$3.0 \times 10^{-3}$	$5.7 \times 10^4$	ref 37
protoFe(III)	$\text{SCN}^-$	$5.9 \times 10^3$	27	$2.2 \times 10^2$	ref 37
protoFe(III)	imidazole	$2.8 \times 10^2$	4.5	$6.2 \times 10^2$	ref 37
protoFe(III)	pyridine	$8.7 \times 10^2$	$1.5 \times 10^2$	5.7	ref 38

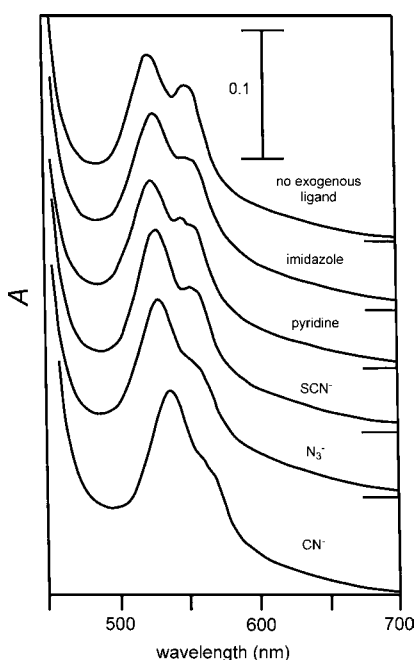


**Figure 6.** Visible absorption spectra of Co(III) Mb derivatives. The protein concentration is identical for all of the samples in 0.1 M Tris buffer at pH 7.0 and 20 °C. The short horizontal lines at 700 nm correspond to the zero absorbance.

**Table 2. Electronic Absorption Spectra of Co(III) DeuteroHeme Mb<sup>a</sup>**

ligand	peak maximum, nm ( $\epsilon$ , $\text{mM}^{-1} \text{cm}^{-1}$ )		
	Soret	$\beta$	$\alpha$
$\text{H}_2\text{O}$	414 (128)	525 (11.4)	552 (9.5)
$\text{OH}^-$ (pH 10.5)	417 (124)	532 (11.6)	556 (8.2)
imidazole	417 (140)	528 (11.9)	551 (9.2)
pyridine	416 (132)	527 (11.6)	548 (9.3), 558 (8.8)
$\text{SCN}^-$	421 (124)	539 (12.3)	555 (8.9)
$\text{N}_3^-$	421 (119)	532 (12.0)	560 (7.9)
$\text{CN}^-$	422 (129)	536 (12.3)	560 (8.2)

<sup>a</sup>In 0.1 M Tris buffer at pH 7.0 and 20 °C.

**Spin-State of Aquomet Co(III) Mb.** Another notable result found in Co(III) Mb derivatives is their mutual spectral similarity. The visible absorption of aquomet Co(III) Mb at pH 7.0 is close to those of the imidazole,  $\text{N}_3^-$ ,  $\text{SCN}^-$  and  $\text{CN}^-$  derivatives (Figure 6 and Table 2). This is in marked contrast with the results in aquomet Fe(III) Mb.<sup>24</sup> The observation

suggests that all of the Co(III) Mb derivatives, including the aquomet protein, may be low-spin.

Since Co(III) has six 3d-electrons, which is identical with Fe(II), two electronic configurations of high-spin ( $S = 2$ ) or low-spin ( $S = 0$ ) are possible in an octahedral coordination environment.<sup>25</sup> It is well-known that Co(III) hemoproteins are EPR-silent, but the observation does not rule out the possibility of the high-spin state for Co(III) Mb because EPR is inactive to both high- ( $S = 2$ ) and low-spin ( $S = 0$ ) states. In contrast, proton NMR discriminates the two states. For instance, in the NMR spectra of Fe(II) Mb, which is high-spin with  $S = 2$ , heme peripheral protons appear in the 50–60 ppm region because the  $3d_{z^2-x^2-y^2}$  orbital in Fe(II) are populated in the high-spin state.<sup>15,26,27</sup> It is then expected that the 2,4-protons of Co(III) deuteroHeme (Figure 1), isoelectronic with Fe(II) deuteroHeme, will also appear in a similar region if it were high-spin ( $S = 2$ ).<sup>15,26,27</sup> However, none of the paramagnetic proton NMR signal are found in Figure S2 in SI. The NMR result excludes the high-spin state, and confirms the diamagnetic low-spin ( $S = 0$ ) assignment for aquomet Co(III) Mb.

One may subsequently ask the reason why aquomet Co(III) Mb is low-spin, whereas aquomet Fe(III) Mb is high-spin, although both of the Mbs are ligated with weak-field ligand  $\text{H}_2\text{O}$ . The answer lies in the molecular structure of Co(III) heme. The X-ray analyses show that the Co(III)–N(pyrrole) bond (1.985 Å) in Co(III)Cl heme is shorter than the Fe(III)–N(pyrrole) bond (2.060 Å) in Fe(III)Cl heme.<sup>28,29</sup> The shorter Co(III)–N(pyrrole) bonds strengthen the equatorial ligand-field to split more the energy-level between the  $t_{2g}$ - and  $e_g$ -type 3d-orbitals in Co(III).<sup>25</sup> Under this circumstance, the low-spin state of aquomet Co(III) Mb is achieved even by the weakly coordinating  $\text{H}_2\text{O}$ . The binding of stronger ligands such as  $\text{N}_3^-$ ,  $\text{CN}^-$ ,  $\text{SCN}^-$ , imidazole and pyridine to aquomet Co(III) Mb accordingly occurs with no change in spin state ( $S = 0$ ). The same is true for the acid-alkaline transition in aquomet Co(III) Mb (Figure 7), which occurs without spin state change. For this reason, the low-spin type of spectra are commonly observed among the Co(III) Mb derivatives (Figure 6).

**Neutral Ligand Binding in Comparison with Fe(III) Mb.** We compared the ligation behaviors between Co(III) and Fe(III) Mbs. In the comparison of Table 1, protoheme Fe(III) Mb, rather than deuteroHeme Fe(III) Mb, was employed as a reference protein because the ligand-binding results for deuteroHeme Fe(III) Mb were not available in literature and because the 2,4-substituent difference between proto- and deutero-hemes,<sup>24</sup> to first approximation, might be less significant than the Co(III) and Fe(III) difference. This assumption is supported by the results that the pK values of

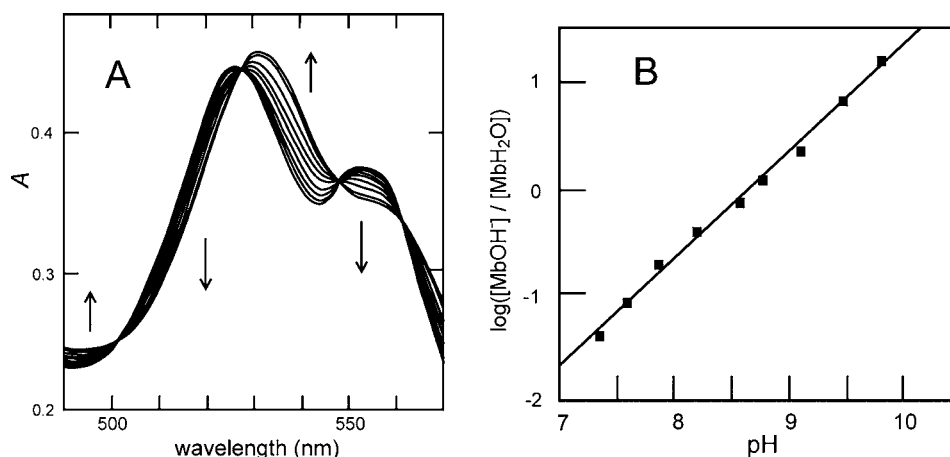


**Figure 7.** Acid-alkaline transition of Co(III) deuteroheme Mb. (A) Visible absorption changes in 10 mM Tris at 20 °C. The arrows indicate increase in pH. (B) Analysis of the absorbance at 540 nm. The transition occurred at  $\text{pH} = 8.70 \pm 0.11$ . The line is the least-squares fit with a slope of 1.0.

the acid-alkaline transition in aquomet deuteroheme Co(III) Mb ( $\text{pK} = 8.70$ ) and aquomet protoheme Co(III) Mb ( $\text{pK} = 8.56$ ) are similar to each other (Figure 7 and Figure S1). Slightly smaller  $\text{pK}$  value in the latter is related to the electron withdrawal effect of heme vinyl groups.<sup>24</sup> The difference between proto- and deuteroporphyrins is thus small.

Table 1 shows that Co(III) Mb exhibits appreciably large equilibrium affinities to pyridine and imidazole, and that the affinities are comparable with or higher than those reported for Fe(III) Mb. It is also important to point out that the  $k_{\text{on}}$  values of Co(III) Mb are approximately 3 orders of magnitude smaller than those of Fe(III) Mb. The acid-alkaline transition of aquomet Co(III) Mb occurs at  $\text{pH} 8.7$ , suggesting the presence of a normal hydrogen-bonding linkage by the coordinating water molecule. Accordingly, the much lower  $k_{\text{on}}$  rates in Co(III) Mb is unlikely to reflect the distortion in the distal coordination environment. One possible explanation for the slow  $k_{\text{on}}$  rates is that Co(III) ion with outermost six 3d-electrons much lowers the access of the basic pyridine and imidazole than Fe(III) ion with five 3d-electrons.

Additional interesting result in Table 1 is that the dissociation rates of the neutral ligands are 6 orders of magnitude smaller than those found in Fe(III) Mb. X-ray analyses showed that the Co(III)–N(imidazole) bond (1.929 Å) is shorter by about 0.04 Å than the Fe(III)–N(imidazole) bond (1.974 Å) in the *bis*-imidazole compounds of Co(III) and Fe(III) teraphenylporphyrins.<sup>28,29</sup> Nakamura and co-workers from the NMR analysis of metallo porphyrins demonstrated that the somewhat shorter Co(III)–N(imidazole) bond led to much stronger metal-imidazole interactions, and that the imidazole dissociation rate dramatically fell down to  $1/10^5$  when the Fe(III) was replaced with Co(III).<sup>30,31</sup> Consistent with their observation, the  $k_{\text{off}}$  rates of the imidazole and pyridine to Co(III) Mb are 6 orders of magnitude smaller than those of Fe(III) Mb (Table 1). The exceedingly smaller  $k_{\text{off}}$  values in Co(III) Mb, as compared with those in Fe(III) Mb, may be interpreted in terms of a shorter Co(III)–N(pyridine) bond. The small  $k_{\text{off}}$  values for pyridine and imidazole compensate the  $k_{\text{on}}$  rates to afford large equilibrium affinities of these ligands to Co(III) Mb.

**Anionic Ligand Binding in Comparison with Fe(III) Mb.** Similar to pyridine and imidazole, extremely small  $k_{\text{off}}$  rates were also found for anionic ligands of  $\text{CN}^-$ ,  $\text{N}_3^-$ , and  $\text{SCN}^-$  in Table 1. Although the results for these anions are not readily

explained, the crystal structures of relevant anion-metal complexes may provide the clue. The Co(III)– $\text{N}_3^-$  distance (1.951 Å) in a *bis*-azide Co(III) teraazamacrocyclic<sup>32</sup> is shorter than the corresponding Fe(III)– $\text{N}_3^-$  distance (1.998 Å) in *bis*-azide Fe(III) heme.<sup>33</sup> The Co(III)–CN distance (1.90 Å in average) in  $\text{K}_3[\text{Co(III)(CN)}_6]$  is also shorter than the Fe(III)–CN distance (1.95 Å in average) in  $\text{K}_3[\text{Fe(III)(CN)}_6]$ .<sup>34</sup> In model heme compounds, the Co(III)–Cl bond (2.149 Å) is shorter than the Fe(III)–Cl bond (2.193 Å).<sup>35,36</sup> Much smaller  $k_{\text{off}}$  rates for  $\text{CN}^-$ ,  $\text{N}_3^-$ , and  $\text{SCN}^-$  in Co(III) Mb (Table 1), in comparison with Fe(III) Mb, may arise from the shorter Co(III)–anion distances and the stronger coordination-bonds.

In summary, the above analyses indicated that Co(III) Mb exhibits characteristic low-spin type electronic spectrum despite the water ligation to Co(III). The kinetic profile is unique in comparison with Fe(III) Mb. We suggest that these differences arise from the properties of Co(III) which is one-electron larger, and which forms shorter metal–ligand bonds than Fe(III) in many inorganic compounds.

## ■ ASSOCIATED CONTENT

### 📄 Supporting Information

The pH-dependent visible spectra of Co(III) protoheme Mb, and the proton NMR of Co(III) deuteroheme Mb. This material is available free of charge via the Internet at <http://pubs.acs.org>.

## ■ AUTHOR INFORMATION

### ✉ Corresponding Author

\*E-mail: [sneya@faculty.chiba-u.jp](mailto:sneya@faculty.chiba-u.jp). Telephone and Fax: +81-43-226-2923.

### 📝 Notes

The authors declare no competing financial interest.

## ■ ACKNOWLEDGMENTS

This work was supported by Grants-in-Aid for Scientific Research from the Ministry of Education, Culture, Sports, Science and Technology Japan, Nos. 23590040 (C), 24249086 (A), and the SPECT program.

## ■ REFERENCES

- (1) Hoffman, B. M. In *The Porphyrins*; Dolphin, D., Ed.; Academic Press, New York, 1979; Vol. 7, pp 403–444.
- (2) Dickerson, C. L. *J. Chem. Educ.* **1976**, *53*, 381–385.

- (3) Chien, J. C. W.; Dickerson, L. C. *Proc. Natl. Acad. Sci. U.S.A.* **1972**, *69*, 2783–2787.
- (4) Basolo, F.; Hoffman, B.; Ibers, J. A. *Acc. Chem. Res.* **1975**, *8*, 384–392.
- (5) Yonetani, T.; Yamamoto, H.; Woodrow, G. V., III *J. Biol. Chem.* **1974**, *249*, 682–690.
- (6) Ikeda-Saito, M.; Iizuka, T.; Yamamoto, H.; Kayne, F. J.; Yonetani, T. *J. Biol. Chem.* **1977**, *252*, 4882–4887.
- (7) Imai, K.; Ikeda-Saito, M.; Yamamoto, H.; Yonetani, T. *J. Mol. Biol.* **1980**, *188*, 636–648.
- (8) Ridsdale, S.; Cassatt, J. C.; Steinhardt, J. *J. Biol. Chem.* **1973**, *248*, 771–776.
- (9) Brucker, E. A.; Olson, J. S.; Phillips, J. N., Jr.; Dou, E. I.; Ikeda-Saito, M. *J. Biol. Chem.* **1996**, *271*, 25419–25422.
- (10) Zahran, Z. N.; Chooback, L.; Copeland, D. M.; West, A. H.; Richter-Addo, G. B. *J. Inorg. Biochem.* **2008**, *102*, 216–233.
- (11) Hambright, P.; Lemelle, S.; Alston, K.; Neta, P.; Newball, H. H.; Stephano, S. D. *Inorg. Chim. Acta* **1984**, *92*, 167–172.
- (12) Moura, J. J. G.; Moura, I.; Bruschi, M.; Le Gall, J.; Xavier, A. V. *Biochem. Biophys. Res. Commun.* **1980**, *92*, 962–970.
- (13) Yoshida, T.; Kikuchi, G. *J. Biol. Chem.* **1978**, *253*, 8479–9482.
- (14) Heinecke, J. L.; Yi, J.; Pereira, J. C. M.; Richter-Addo, G. P.; Ford, P. C. *J. Inorg. Biochem.* **2012**, *107*, 47–53.
- (15) Goff, H. In *Iron Porphyrins*; Lever, A. B. P., and Gray, H. B., Eds.; Addison-Wesley, London, 1983; Part I, pp 237–281.
- (16) Fuhrhop, J.-H., and Smith, K. M. In *Porphyrins and Metalloporphyrins*; Smith, K. M., Ed.; Elsevier, Amsterdam, 1975; pp 773–835.
- (17) Janson, T. R., and Katz, J. J. In *The Porphyrins*; Dolphin, D., Ed.; Academic Press, New York, 1979; Vol. 4, pp 1–59.
- (18) Adler, D.; Longo, F.; Kampas, F.; Kim, J. *J. Inorg. Nucl. Chem.* **1979**, *32*, 2443–2445.
- (19) Asakura, T. *Methods Enzymol.* **1978**, *52*, 447–455.
- (20) Neya, S.; Tsubaki, M.; Hori, H.; Yonetani, T.; Funasaki, N. *Inorg. Chem.* **2001**, *40*, 1220–1225.
- (21) Bernasconi, C. F. *Relaxation Kinetics*; Academic Press, New York, 1976, pp 11–19.
- (22) Smith, D. W., and Williams, R. J. P. In *Struct. Bonding (Berlin)*; Hemmerich, P., Jorgensen, C. K., Neilands, J. B., Nyholm, S. R. S., Reinen, D., and Williams, R. J. P., Eds.; Springer Verlag, Berlin, 1972; Vol. 7, pp 1–45.
- (23) Sliger, S. G. *Biochemistry* **1976**, *15*, 5399–5406.
- (24) Tamura, M.; Woodrow, G. V., III; Yonetani, T. *Biochim. Biophys. Acta* **1973**, *317*, 34–49.
- (25) Shriver, D. F., Atkins, P. W., and Langford, C. H. *Inorganic Chemistry*, 2nd ed.; Oxford University Press, Oxford, 1994; pp 226–273.
- (26) Neya, S.; Funasaki, N.; Sato, T.; Igarashi, N.; Tanaka, N. *J. Biol. Chem.* **1993**, *268*, 8935–8942.
- (27) Scharberg, M.; La Mar, G. N. *J. Am. Chem. Soc.* **1993**, *115*, 6513–6521.
- (28) Lauher, J. W.; Ibers, J. A. *J. Am. Chem. Soc.* **1974**, *96*, 4447–4452.
- (29) Collins, D. M.; Countryman, R.; Hoard, J. L. *J. Am. Chem. Soc.* **1972**, *94*, 2066–2072.
- (30) Nakamura, M. *Bull. Chem. Soc. Jpn.* **1995**, *68*, 197–203.
- (31) Saitoh, T.; Ikeue, T.; Ohgo, Y.; Nakamura, M. *Tetrahedron* **1997**, *53*, 12487–12496.
- (32) Sakurai, T.; Yamamoto, K.; Naito, H.; Nakamoto, N. *Bull. Chem. Soc. Jpn.* **1976**, *49*, 3042–3046.
- (33) Hoard, J. L.; Cohen, G. H.; Glick, M. D. *J. Am. Chem. Soc.* **1967**, *89*, 1992–1996.
- (34) Vannerberg, N. G. *Acta Chem. Scand.* **1972**, *26*, 2863–2876.
- (35) Cho, J.; Kim, J. C.; Lough, A. J. *Inorg. Chem. Commun.* **2003**, *6*, 284–287.
- (36) Ellison, M. K.; Hasri, H.; Xia, Y.-M.; Marchon, J.-C.; Schultz, C. E.; Debrunner, P. G.; Scheidt, W. R. *Inorg. Chem.* **1997**, *36*, 4804–4811.
- (37) Antonini, E., and Brunori, M. *Hemoglobin and Myoglobin in Their Reactions with Ligands*; North-Holland, Amsterdam, 1971, pp 229–234.
- (38) Chen, Y.; Liu, G.; Tang, W. *Inorg. Chim. Acta* **1996**, *249*, 239–243.